CEAS-GNC-2024-045

EuroGNC Navigation Guidance Control CEAS Bristol, UK June 11th-13th 2024
University of BRISTOL ROYAL AERONAUTICAL SOCIETY AIAA

Fault-Tolerant Control for a Cluster of Rocket Engines – Results for launch and landing of a re-usable launcher

Cristina Roche Arroyos GNC Engineer, GMV, 1990-392, Lisbon, Portugal. Cristina.Roche@gmv.com

Matteo Pascucci GNC Engineer, GMV, 1990-392, Lisbon, Portugal. Matteo.Pascucci@gmv.com

Nuno Paulino Senior Engineer, GMV, 1990-392, Lisbon, Portugal. Nuno.Paulino@gmv.com

Jorge Arnedo GNC Engineer, GMV, 28760, Madrid, Spain. Jarnedo@gmv.com

Diego Navarro-Tapia *Senior Research Associate, Universidad Carlos III de Madrid, Aerospace Eng. Dept., 28911, Madrid, Spain [The work presented was peformed when author was senior engineer at Technology for Aerospace Control Ltd (TASC), UK]*

Andrés Marcos *Beatriz Galindo Senior Distinguished Investigator, Universidad Carlos III de Madrid, Aerospace Eng. Dept., 28911, Madrid, Spain[The work presented was peformed when author was scientific director of Technology for Aerospace Control Ltd (TASC), UK]*

Mohamed Lalami Senior system Control, Actuation Business unit SABCA, 1470 Belgium, Mohamed.Lalami@sabca.be

Paul Alexandre Actuation systems Expert, Actuation Business unit SABCA, 1470 Belgium, Paul.Alexandre@sabca.be

Pedro Simplício GNC Engineer, Aurora Technology for ESA-ESTEC, Keplerlaan 1, 2201 AZ Noordwijk, Netherlands. Pedro.Simplicio@ext.esa.int

Massimo Casasco Head of the Guidance, Navigation and Control Section, ESA-ESTEC, Keplerlaan 1, 2201 AZ Noordwijk, Netherlands. Massimo.casasco@esa.int

ABSTRACT

The project entitled "Fault-Tolerant Control of Clusters of Rocket Engines (FTC-CRE)" was an activity supported by the European Space Agency aimed at the demonstration of guidance and control (G&C) laws for launch vehicles with cluster of engines, with focus on reconfiguration capabilities in case of propulsion and Thrust Vector Control (TVC) failures. The analyzed scenario covered the entire trajectory of the first stage, encompassing the Ascent phase of the complete vehicle from take-off to separation, as well as the Descent for the first stage reusability, which includes the re-entry and landing burn of the detached first stage. The objectives of this project were to study and define suitable requirements and to propose and demonstrate valid methodologies for guidance and control architectures with embedded fault tolerant capabilities. In addition, the project required to demonstrate the increase in readiness level for recovery strategies in the presence of failures in terms of stability and performance. This article provides an overview

of the activity, the description of launcher benchmark, and a summary of the results and findings attained in the project, which concluded in December 2023.

Keywords: Guidance and Control, Fault-Tolerant Control, Re-entry, Reusable Launcher, Successive Convexification Trajectory Generation, Thrust Vector Control, TVC Allocation Pseudo-Inverse, TVC Failure, Propulsion Failure, Cluster of Rocket Engines, Onboard Guidance.

Nomenclature

DoF	Degrees of Freedom
EMA	Electromechanical actuator
ESA	European Space Agency
FDIR	Failure Detection Isolation and Recovery
FES	Functional Engineering Simulator
FTC	Fault-Tolerant Control
FTC-CRE	Fault-Tolerant Control of Clusters of Rocket Engines
G&C	Guidance and Control
IB	Intermediate Burn
LB	Landing Burn
LFT	Linear Fractional Transformation
LFT	Linear Fractional Transformation
LP	Landing Pad
LTI	Linear Time Invariant
LVM	Launch Vehicle Manager
MC	Monte Carlo
MECO	Main Engine Cut-Off
PD	Powered Descent
RCS	Reaction Control System
SCvx	Successive Convexification
TVC	Thrust Vector Control
w.r.t	with respect to

1 Introduction

In the last quarter of the century most launcher mission failures were caused by loss of propulsion or failures in Thrust Vector Control (TVC). The former involves an off-nominal thrust delivery causing insufficient delta-V, leading to a failure to reach orbit or an off-nominal orbital injection performance. Moreover, in the case of TVC, a reduction in thrust also leads to a reduction in control authority. The use of Fault-Tolerant Control (FTC) functions for launch vehicles is nowadays mostly passive, based on hardware redundancy (e.g. Ariane 5 launcher [1]), with limited active FTC adoption and mainly based on ad-hoc solutions (e.g. VEGA launcher [3]), and advanced control techniques such as the adaptive augmentation control scheme used by the SLS [4], which is shown to augment the envelope of the mission and avoid potential loss of vehicles. However, the redundancy provided by the cluster of engines can be intelligently exploited to mitigate failures that affect propulsion or thrust vectoring.

FTC for a cluster of engines in launchers has regained attention, notably with the development of capabilities in new reusable launchers like SpaceX Falcon 9 and Starship. Partially or fully reusable launch vehicles are being studied in preparation for the future of launch systems. The increased complexity of that vehicle scenario is not only evident in design and architecture but also poses a distinct challenge in G&C. While Europe has a rich heritage of developing tools like DIAMANT, EUROPA, and ARIANE for expendable launchers, adapting them for reusable launchers and re-entry flight is not always seamless. The need for novel approaches and tools tailored to the unique demands of reusable systems becomes imperative in ensuring the success and efficiency of re-entry G&C for future launch systems.

This paper presents an overview of the "Fault-Tolerant Control of Clusters of Rocket Engines (FTC-CRE)" activity [1], supported by the European Space Agency (ESA) and its main results, based on a test case of a 2-stages micro launcher of 25m length and 1.8m diameter, 32 tones wet mass, mounting a cluster of 5 liquid engines turbine-fed that deliver 83.3 kN each, and considering the 1st stage reusable with propelled vertical landing. The study encompasses the Ascent flight of the full vehicle, from take-off to separation and it also includes the development of tailored G&C and recovery algorithms for the re-entry flight of the 1st stage, also covering the landing burn at the land site. The study considers both a baseline scenario and variations subjected to common propulsion and TVC failures. The non-linear simulator includes a developed high-fidelity model of the TVC electro-mechanical actuator, and the capability to inject propulsion and TVC failures. A recovery decision logic is proposed relying on dynamic TVC allocation, FTC, a more aggressive TVC inner-loop controller and the capability of trajectory reconfiguration using Successive Convexification (SCvx). The recovery actions are tested and analyzed with the simulator for Ascent, re-entry and landing phases, to derive requirements and methodologies for a G&C architecture with embedded fault-tolerant capabilities, increasing the readiness level for recovery strategies.

The paper is organized as follows: Section 2 provides a summary of the launcher system, mission and Functional Engineering Simulator (FES) developed; Section 3 briefly describes the approach for the baseline nominal G&C; Section 4 provides a description of the failure analysis followed by the proposed recovery actions and a summary of the test campaigns carried out in the project; Section 5 provides some of the results and their discussion; Section 6 summarizes the main points of the activity and conclusions.

2 Mission and System

The case study presented in this paper has been selected to be a representative launcher case. Its design has been iterated in collaboration with ESA across several past projects to reflect a broad range of potential clustered TVC launchers. The activity is focused on the 1st stage flight, including the *Ascent* phase of the full vehicle up to separation, and the *Descent* and landing of the separated stage. The 1st stage is powered by a 5-engines cluster arranged in cross shape, with each outer engine actuated by 2 TVC actuators, as depicted in in Figure 1 on the right side.

The reference trajectory is generated using an internal trajectory optimization tool developed by GMV. The optimal trajectory, starting from Kourou Launch Base, is designed to reach the objective sun-synchronous target orbit while minimizing the consumed fuel. The main requirements for the Ascent mission include ensuring the product of dynamic pressure and the angle of attack (Qα) shall below 80 kPaº, to maintain launcher structural integrity. The roll rate shall be lower than 5º/s to consider the coupling dynamics between pitch and yaw attitude negligible, and allow for separate control channels of pitch and yaw [12][18]. As for the reference Descent trajectory, a downrange scheme is selected with two propelled phases, intermediate and landing burn, connected by an aerodynamic phase, as depicted in the left plot of Figure 1. The reference trajectories for both burns are generated using SCvx and considering 6-DoF and the total available propellant mass. Deployed fins can also be used also for aerodynamic control, to be defined depending on the application. In this case study, aerodynamic control is not addressed, and the propelled phases are designed considering the worst-case scenario of static fins, which don not aid the TVC.

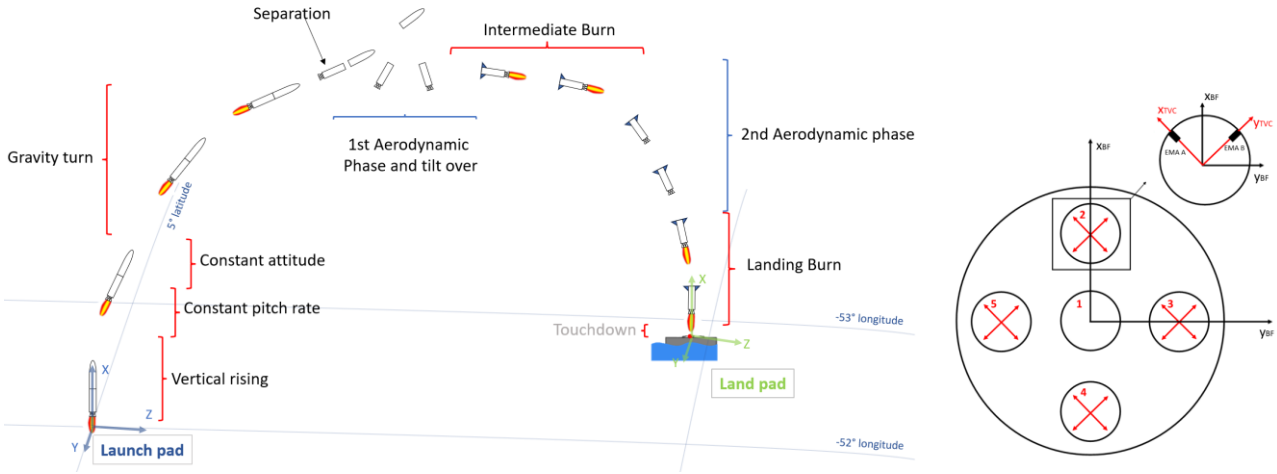

Figure 1 Mission phases (left); TVC actuators and cluster of engines configuration in Body Frame (right).

The G&C and recovery algorithms are analyzed and validated within a FES developed and implemented in Matlab/Simulink, including gravity gradient torque, gravitational acceleration with J2 perturbation, wind and atmospheric models, and aerodynamic loads. The actuation comprises a propulsion system, responsible for computing thrust force and mass consumption, 2 TVC actuators per outer engine, and 8 reaction thrusters for roll rate control. The TVC simulator utilizes a Multiphysics Simscape model, featuring an actuation system with two electromechanical actuators (EMAs), control and power electronics, and the power supply (battery). The TVC model can simulate faults of electrical or mechanical components leading to loss of power or the stuck of an actuator. The model includes the permanent magnet synchronous motor, gearbox, ball screw, power switches, sensors, software controller and nozzle dynamics. TVC nominal behavior was validated using real test data from SABCA's EMAs.

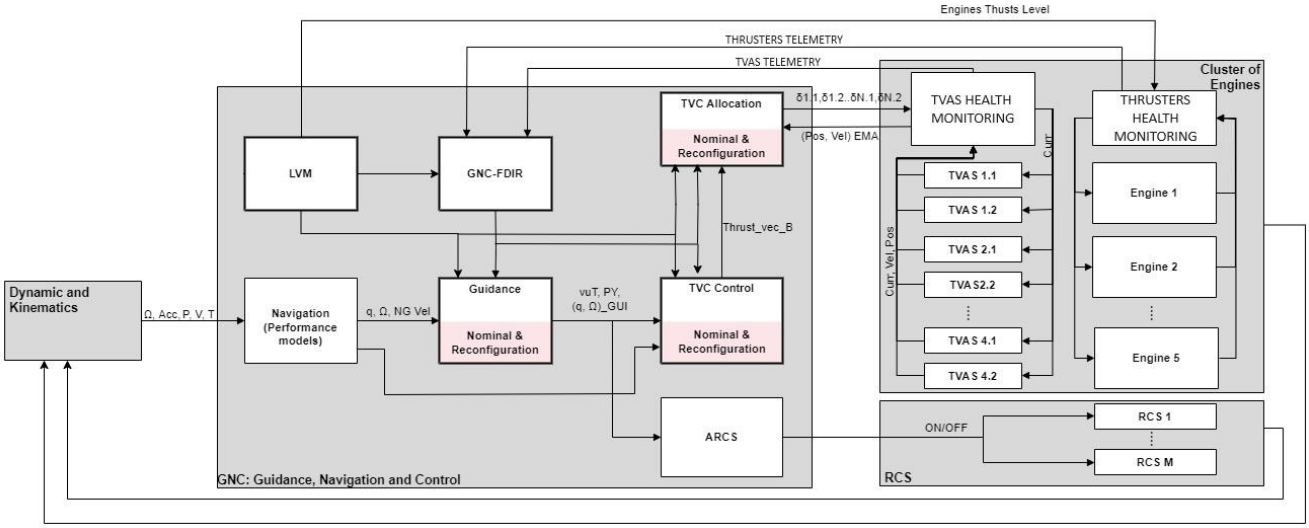

Figure 2 Schematic block diagram of the baseline FES and G&C system.

The Guidance function provides the flight control with launcher reference attitude (pitch and yaw angles), position and velocity as decided by the Launch Vehicle Manager (LVM). The Control computes TVC deflections and thrust levels for attitude and trajectory tracking. The Failure Detection Isolation and Recovery (FDIR) function, receiving telemetry from TVC and engines, triggers the recovery actions.

3 Baseline Guidance and Control

Algorithms for G&C under conditions without failures were designed and validated as a baseline for comparison and to assess the impact of the modelled failures and the recovery strategies. The analysis focuses on control authority and performance, and dispersions at the end of the Ascent flight and landing. The G&C validation is carried with Monte Carlo (MC) campaigns under parametric dispersions.

The Ascent baseline guidance uses an open-loop scheme scheduled with non-gravitational velocity, a common approach for endo-atmospheric guidance due to its simplicity compared with closed-loop schemes [12][17].

The baseline Descent guidance covers the 1st stage flight from separation to the target Landing Pad (LP). Unlike the Ascent trajectory, Power Descent (PD) trajectories exhibit a broader range of angles of attack, and rocket engines operate in a throttleable manner rather than continuously at maximum thrust. For Descent trajectories of reusable launchers, precise final states with minimal deviations and uncertainties are crucial to land at the predetermined pad location. Therefore, it is required that the guidance outputs optimal position and velocity variables, in addition to attitude. Furthermore, to compensate for deviations, the baseline Descent guidance needs a closed-loop implementation. The Descent trajectory incorporates an initial aerodynamic phase, Intermediate Burn (IB), and a subsequent aerodynamic phase, reaching maximum dynamic pressure, followed by the Landing Burn (LB), as shown in the left plot of Figure 1. The study on reconfiguration under propulsion failures during Descent is conducted on the propelled phases, LB and IB.

A python formulation for SCvx was developed, analyzed, and integrated in the FES for IB and LB guidance scenarios. The algorithm is initialized with landing point estimation and IB initial conditions to adapt to the conditions resulting from variations in the Ascent phase. Numerical challenges of the solver are addressed through thorough scaling of optimization variables, resulting in solutions that converge

independently of parameters and initial guesses. The feasibility of these converged solutions is demonstrated with nonlinear propagation and the FES, validating SCvx required modelling simplifications. New constraints representing launcher dynamics are developed, and the final cost function is tuned for fast convergence to a feasible, locally optimal solution. The SCvx solution for Descent baseline guidance, later applied to reconfiguration guidance for Ascent (*R4* in Section 4), is an efficient and tailored collection of strategies and self-developed contributions targeting the system.

The cluster configuration results in an over-defined application of control torque, with redundant configurations of the deflections of the 4 outer nozzles. A baseline engine allocation unit determines each engine's contribution to the total moment torque for attitude and drift control. The allocation algorithm uses a high-efficiency quasi-linear approach based on a weighted Least Squares generalized inverse and augmented with a null-space method [5]. Roll control is out of the focus of the study, and a logic-based RCS limits the roll rate using 8 reaction thrusters symmetrically positioned around the cross section.

For control design (yaw, pitch and drift), the synthesis uses operational points along the nominal trajectory to obtain a linear structured $\mathcal{H}_\infty$ controller, with parameters which can be scheduled throughout the flight. Linear Time Invariant (LTI) and Linear Fractional Transformation (LFT) mathematical models for design are defined for the linearized dynamics of the rocket launcher along points of the trajectory, under the usual assumptions of small angles approximation for the propulsion force and torque, axis-symmetrical rocket, limited roll rate and a gravity turn trajectory [7]. This control design approach, extensively applied over the last years robust control of rocket launchers [8], leverages the advantages of the $\mathcal{H}_\infty$ framework in robust control design and analysis for linear systems. LTIs and augmented plants are defined for each pitch and yaw channels to address attitude and drift control. Controller synthesis involves fine-tuning weighting functions of the augmented plant, achieving a suitable tradeoff between attitude, drift, and aerodynamic loads 0 (with a focus on Qα for vehicle load relief [9]), while ensuring stability. After the synthesis, the LFTs are used with μ-analysis [6] to assess robust stability and performance against requirements under uncertainty.

For Descent phases, the lateral control synthesis follows the same methodology as for the Ascent phase, focusing on drift and position control. Additionally, a longitudinal controller is added to track the guidance Descent velocity profile, enhancing the rocket's autonomous adaptation to off-nominal conditions through throttle capability and assisting in achieving a feasible vertical velocity for landing.

4 Failure Analysis, Scenarios and Recovery Actions

Table 1 Failure and recovery actions considered for the different propelled phases.

Failures considered and modelled				Recovery actions studied		
Type	Affected engine	Details	Id	Ascent burn	Descent phase	
					Intermediate burn	Landing burn
Loss of thrust	Central	< 40%	F1	R1		
		> 40%	F2	R1, R3	R1	
	Outer	< 40%	F3	R1		
		∈ [40-70] %	F4a	R1, R2, R3, R4		
		> 70%	F4b	R1, R4	R1, R3	R1*

Jamming of TVC	Outer	At non-zero deflection	F5	R1, R3	R1	
Loss of TVC power	Outer	Static disturbance load	F6a	R1	R1, R3	
		Dynamic vibration	F6b	R1		

Most mission failures in the last quarter-century resulted from propulsion failures (50%), followed by GNC issues (15%, which includes actuator failures), and separation problems (5%) [16]. This work considers realistic failures in one of the cluster's engines as well as thrust vectoring failures. As the objective of this study is to develop fault-tolerant G&C algorithms, the considered failures are those that degrade launcher performance without being catastrophic. The modelled failures include loss of thrust as a propulsion failure with different levels of severity and two severe failures for the TVC actuator:

I. **Propulsion failures: partial and total loss of thrust in one engine (*F1-F4*)**:

Ignoring catastrophic failures (e.g. an engine chamber breach), propulsion failures typically involve partially or totally off-nominal thrust delivery by the propulsion system, (see Table 1). Faults in the central and outer engines are differentiated because the latter result in additional torque deviations on top of force ones (thrust), due to the geometrical off-center configuration, see Figure 1. Observable fault effects were observed at 60% loss of thrust. Considering engine characteristics and recovery actions, thrust loss was modelled with bounds of 40% and 70% by introducing failures in oxidizer and fuel injection valves.

II. **TVC failures:** simulated in a detailed multi-physics Simscape-based TVC actuator model:
   a) **Jamming of TVC (*F5*)**: modelled as one EMA stuck at a fixed non-zero position in an outer engine (loss of communication, avionic failure or any jamming-like behavior), leading to a non-zero deflection of one degree of freedom of one engine.
   b) **Loss of power of TVC (*F6*):** loss of power of the thrust vector actuator in an outer engine; modelled as having one EMA free to move, leading to one degree of freedom of one engine uncontrolled. Besides the case of force eccentricity and quasi-static acceleration, pushing the engine to one of its ends of stroke, it was also investigated the impact of dynamic vibration on the free TVC.

At the control and guidance level, the investigated recovery strategies rely on control reconfiguration and trajectory re-planning based on the detected failure, and were defined as:

- ***R1*:** allocation algorithm to reassign the thrust levels and optimize deflections within the cluster to compensate for the loss of thrust, TVC failures and any induced parasitic torque [10]. *R1* design uses the pseudo-inverse solution, which was modified here for fault-tolerant purposes.
- ***R1**:** reassignment to healthy engines in case of loss of thrust to provide the recovery of optimal thrust and torque authority, while also considering the undesired induced lateral forces.
- ***R2*:** replaces the baseline TVC controller by an FTC-based controller designed by TASC to be robust against propulsion failures. The FTC control design problem is formulated in the structured $\mathcal{H}_\infty$ control framework using the closed-loop interconnection that includes the key features for TVC launcher control design framework proposed in [11] and [12].
- ***R3*:** TVC inner-loop control gains change (*R3*) for a temporarily stressed yet higher-performance TVC.
- ***R4*:** onboard guidance trajectory re-computation modeling fault dynamics. R4 considers a change of trajectory, from the nominal to the reconfigured one, at the time occurrence of the failure (initial states).

The last (*R4*) trajectory reconfiguration guidance is obtained by solving the optimization problem using SCvx. The approach expands on the same technique as the developed baseline guidance for Descent

(see Section 3), due its ability to address the nonconvex and nonlinear nature of the problem while making it amenable for closed-loop online implementation. It includes the constraints and adaptive goals of Ascent flight, along with the modelling of propulsion failures in the cluster. The SCvx guidance logic and problem formulation for *R4* are based on [14], with contributions from [13] and [15]. The SCvx solution for *R4* results from an efficient and tailored collection of strategies and self-developed contributions that entailed multiple design iterations with the FES to ensure non-linear representativeness and feasibility.

Table 1 compiles the scenarios and respective recovery actions analysed and assessed through MC campaigns in the FTC-CRE project. The reader is referred to [1] for more details about the recovery strategies evaluated in this article. Figure 3 depicts the severity of the modelled failures per flight phase.

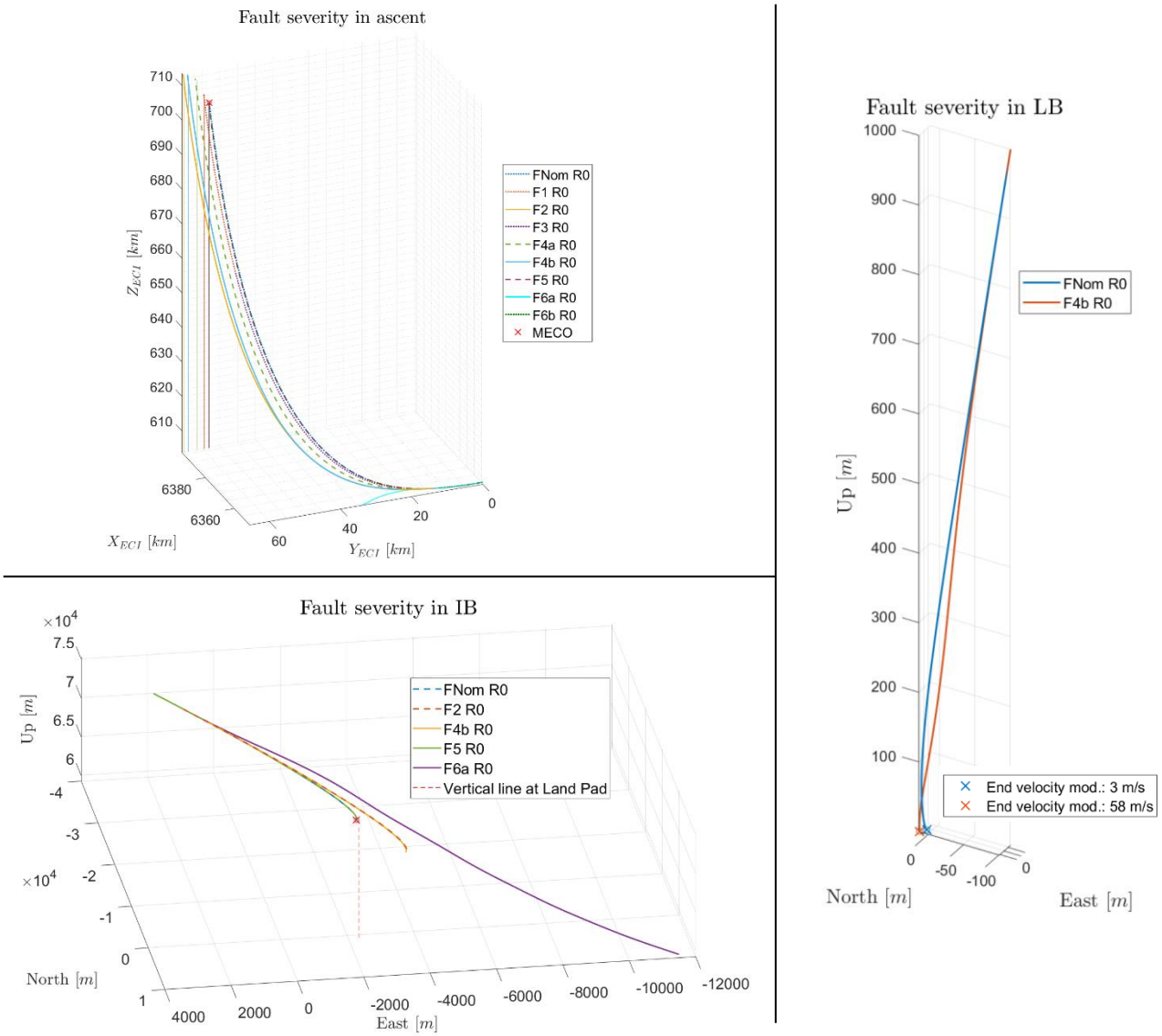

Figure 3 Fault severity per propelled flight phase. <u>Top left:</u> Ascent flight. The red cross represents Nominal MECO coordinates for successful orbit injection. Fault F6a leads to a loss of vehicle, and the high error in translation and velocity at MECO, caused by the failure scenarios F1, F2, F3, F4a, and F4b, leads to a failed orbit injection. The divergence increases with the percentage of thrust loss. <u>Top bottom</u>: IB. The red cross represents the endpoint of the nominal IB, and the red dashed line indicates the vertical at the Land Pad. It can be seen how F6a directly leads to a loss of control of the vehicle, and F2 and F4b failures lead to overpassing the LP or arriving at it with excessive horizontal velocity, therefore resulting in mission failure and no recovery of the first stage. F5 virtually does not affect, since during IB, the TVC activity is low, and torque can be compensated. <u>Right plot</u>: LB. The propulsion failure F4b leads to a catastrophic landing with a touchdown velocity of 58m/s.

5 Campaign results and discussion

The verification and validation campaigns were carried out using the nonlinear FES described in Section 2, integrating the developed baseline and recovery G&C and FTC functions. Simulations considered parametric dispersions in launcher and environmental properties, Earth gravity gradient torque, Earth higher order harmonics limited to J2, wind and turbulence effects, sloshing, navigation performance models, and the Multiphysics TVC model. Bending modes are out of the scope of the study. The MC campaigns comprised 100 cases each, with scenarios split between Ascent and Descent flight phases, to serve as an assessment for the recovery actions performance in such broad type of scenarios.

Due to length restrictions, this section presents only 2 Ascent and 2 Descent campaigns. Additional outcomes, including extra campaigns from Table 1, are discussed in the conclusion. The results display the dispersion envelopes in time domain through key performance indicators. They offer a comparison of the baseline non-faulty case (*MC-F0-0-R0*) as reference (see blue solid lines) w.r.t a failure scenario campaign using recovery strategies. Pitch and yaw errors, and drift are expressed in the launcher body-frame. The TVC deflection plot shows both TVC deflections per engine.

5.1 Loss of EMA power in outer engine (*F6*) during Ascent with *R1* recovery

The aim of this MC campaign is to assess the effectiveness of the dynamic TVC allocation *R1* recovery function to handle TVC loss of power failures. As shown in Figure 4, the TVC loss of power results in a large deviation of the faulty TVC actuator until reaching the TVC maximum deflection (i.e. 10 degrees), see red solid lines in TVC deflections engine 2 plots. The results show that *R1* provides recovery by performing dynamic TVC allocation (see different and higher TVC deflections for the faulty case). In addition, *R1* w.r.t. the baseline non-faulty case roughly presents minimal deviations for the main trajectory parameters (altitude, mass, thrust profile, axial vehicle velocity) as well as for the Qα profile. Also, *R1* further improves pitch attitude and drift responses. It is also observed that one of the TVC actuators of engine 5 reaches saturation in 13 cases. This aspect causes a significant degradation of the roll-rate responses for these specific cases. Some cases of TVC loss of power lead to more severe consequences because the direction in which the TVC gets stuck creates torques of varying difficulty to compensate for, owing to the cluster geometry. In terms of deviations observed at Main Engine Cut-Off (MECO), *R1* can recover enough authority and reach the separation point with small feasible deviations. Overall, the results show that the use of dynamic allocation approach is effective handling TVC actuator failures such as loss of power.

5.2 Partial loss of 60% thrust in outer engine 2 during Ascent, with different combinations of recovery actions

For some failure cases, the failure degradation could not be recovered by a single recovery action, and hence, different combinations of recovery strategies were tested. For instance, propulsion failures above 40% (e.g. F4a in Table 1) cannot be completely compensated via *R1* recovery due to the 110% throttling constraint of the employed engines. Different combinations of recovery actions were explored: a) *R1+R2*; b) *R1+R2+R3*; c) *R1+R2+R4*. Figure 5 illustrates that none of the set of recovery functions can reach the baseline non-faulty total thrust profile (see bottom-right plot), causing a reduction in the axial vehicle velocity and altitude. The combination of *R1* and *R2* gathers the benefits of *R1* to alleviate the loss of thrust in engine 2 by increasing the throttling of the healthy engines at their maximum capacity

and of *R2* that provides significant drift/drift-rate reduction by design. This improvement comes at the expense of higher $Q\alpha$ profile which clearly reflects the underlying competing trade-off objectives. It is also observed that *R1* commands higher TVC deflections to compensate the parasitic torques caused by the mismatch between axis-symmetric engine thrust levels. It is also noted an increase of the roll-rate profile with respect to the baseline non-faulty case, particularly around the maximum $Q\alpha$ region.

The introduction of *R3* provides approximately the same responses as the *R12* recovery function.

Finally, the addition of a guidance reconfiguration and trajectory re-computation *R4* in combination with *R1* and *R2* maintains the advantages of *R12* while providing overall less attitude errors with respect to *R12* and more importantly, it further improves the aerodynamic loads responses presenting lower peaks at maximum $Q\alpha$ region. *R4* was designed attempting to diminish the interaction between changes in the guidance profile and the control function by adjusting the original trajectory to make it feasible under the failure dynamics, however, its interaction with the controller must be further assessed. Due to the difficulties in defining a convex MECO conditions cost function in SCvx, *R4* creates slight deviations in the final translational states, which could be mitigated by considering the exo-atmospheric flight in the optimization problem. This aspect was beyond the scope of the study.

5.3 Total loss of thrust in outer engine 2 during Descent in the Intermediate Burn phase, recovered with *R1*

Compared to Ascent flight, Descent offers more thrust available to compensate for a propulsion failure in one engine. During the IB flight, the total loss of thrust of one engine can be almost fully recovered by throttling the other 4 at 110%, recovering significant thrust authority. This results in a slightly longer IB flight in propulsion failure scenarios, as shown in Figure 6. However, when engines reach saturation, the longitudinal controller action cannot compensate for dispersions. This leads to a 3% position divergence at the end of the IB. This deviation should be compensated in the aero phase and LB or otherwise by a redesign of the IB trajectory to work using less total thrust in the nominal case.

Lateral engine failure (*F4b*) recovered with *R13* achieved similar performance to the nominal but introduced an offset pitch error, slightly degrading performance compared to central engine loss of thrust failure. As expected, the asymmetric configuration caused increased TVC deflection activity and an elevated roll rate due to parasitic torque from undesired lateral forces. The use of *R1* recovery function alone successfully recovered 98% of cases, with the remaining 2% failing due to TVC deflection saturation. Notably, adding *R3* enabled recovery in the 2 previously failing cases, achieving a 100% success rate. This suggests that a TVC actuator model with a higher bandwidth might assist in certain cases of TVC deflection saturation, although this observation was not consistent across all campaigns.

5.4 Total loss of thrust in outer engine 2 during Descent, in the final Landing burn, with recovery action *R1**

The baseline LB campaign shows robustness against parameters dispersion and sloshing, with performances close to the nominal and an accurate tracking of the reference. Thrust authority recovery is crucial for safe landing, and absence of reconfiguration in this phase would result in a catastrophic touchdown. Comparing with Ascent and IB phases, there is engine redundancy during the LB and more thrust available to compensate for propulsion failures. Among the *R1** configurations tested, the best allocation logic in thrust and torque authority recovery is the one illustrated in the results (*R1**) in Figure

7. In this scenario, after failure detection and during ignition transient, parallel engine 4 is active at its maximum, to recover thrust authority. Engines 3 and 5 are ignited post-failure detection, and once they provide effective thrust, engine 4 turns off, leaving the LB with the symmetric pair of engines 3 and 5.

The designed G&C architecture provides soft- and vertical landing performance capable of withstanding wind and loss of thrust failure in an engine. However, wind poses a significant hazard for the LB, causing excessive roll rates. An enhanced version of *R1*, considering lateral forces minimization, or a more powerful RCS could help mitigate this issue. Similar to the baseline scenario, maximum wind induces East drift and drift rate errors due to controller compensation for attitude error. The high thrust-to-weight ratio drives the choice of using 2 engines, contributing to roll rate. While TVC EMAs for engines 3 and 5 saturate, emphasizing the need for additional attitude control during LB, neither saturation nor high roll rates induce instability. This results in only one failed case, consistent with the baseline campaign under the same wind intensity.

In addition, unlike for Ascent and IB campaigns navigation performance models are representative, LB navigation requires more precise set of sensors and advanced filtering techniques whose performance impacts significantly the controller states and guidance profile scheduler and required a dedicated study out of scope for this activity. Thus, LB campaigns are performed assuming ideal navigation.

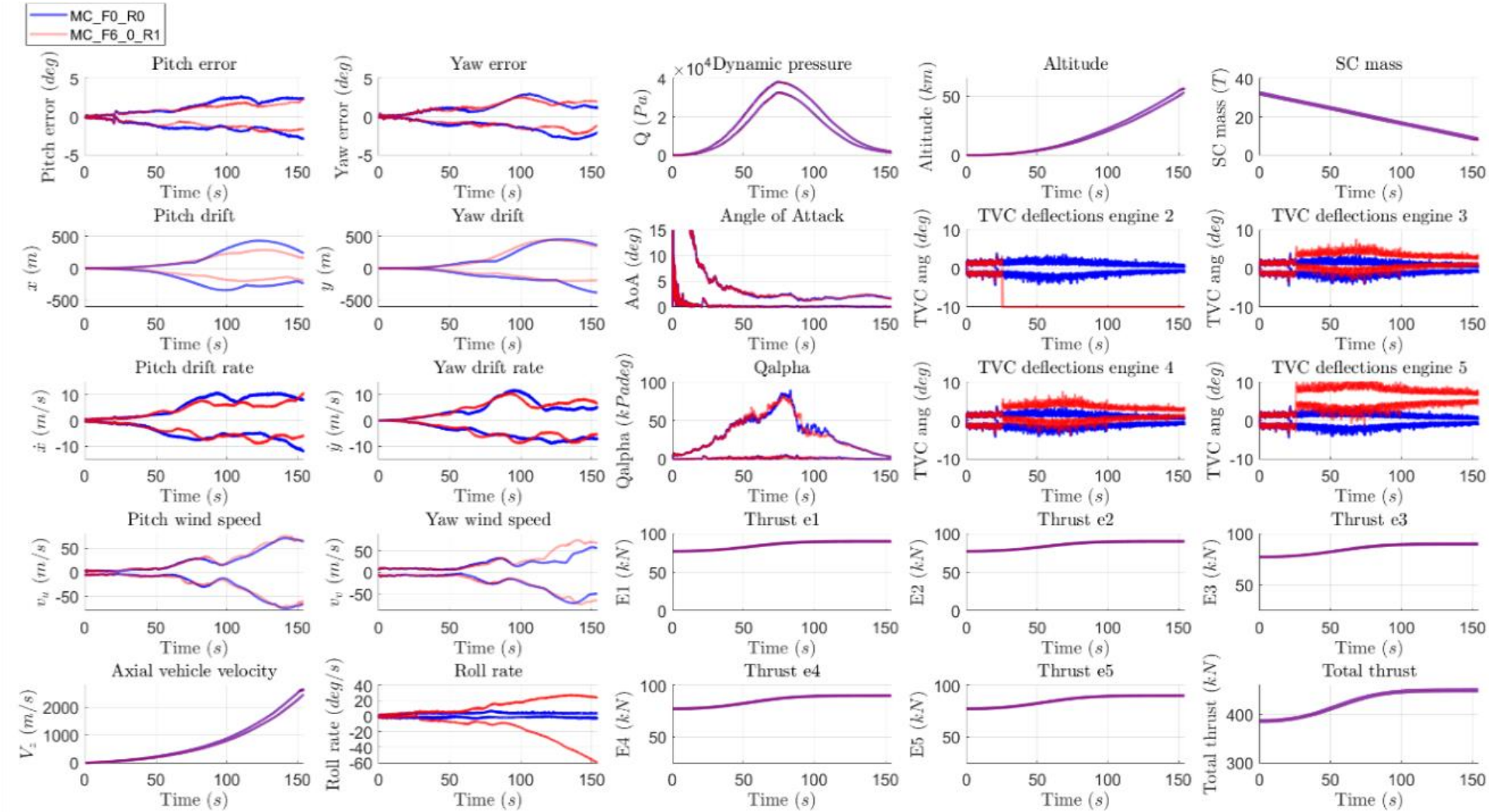

Figure 4 Envelopes of the time histories MC campaigns for 100 cases in Ascent flight. In blue, *MC-F0-0-R0* represents the baseline scenario without failures; in red, *MC-F6-0-R1* shows the envelope of the results when a loss of power in TVC type of failure occurs in an outer engine, the recovery action applied in this scenario is the dynamic TVC allocation (*R1*).

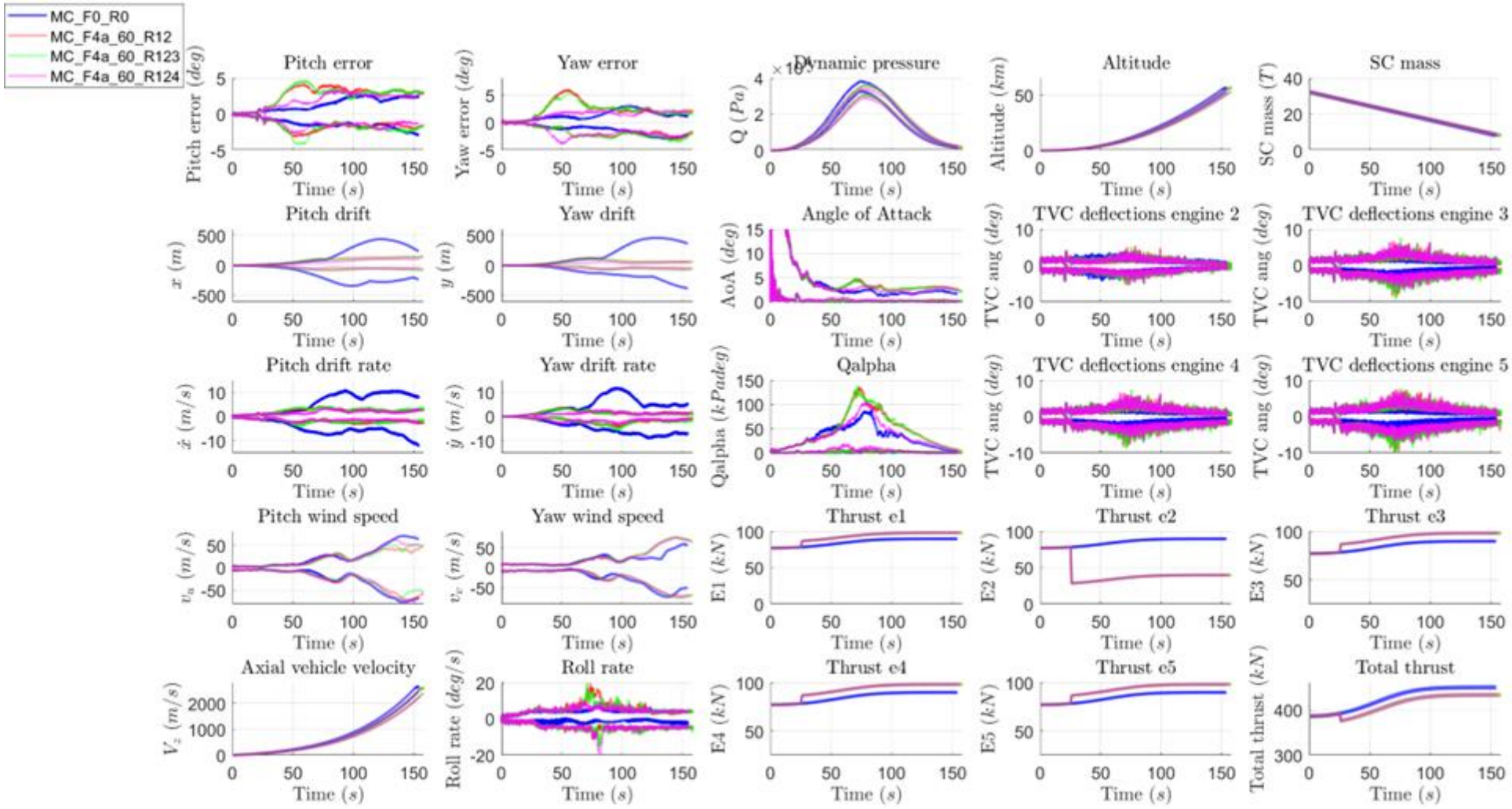

Figure 5 Comparison of the time history envelopes of MC campaigns for 100 cases in Ascent flight. In blue, *MC-F0-0-R0* represents the baseline scenario without failures; in red, green and purple MC campaigns with 40% loss of thrust in an outer engine recovered with different strategies: in red, *MC-F4a-60-R12* recovered with dynamic TVC allocation (*R1)* and an FTC-based controller *(R2)*; green envelope *MC-F4a-60-R123* adds to the previous red option (*R1R2*) the change in TVC inner-loop control gains (*R3)*, while the campaign in purple *MC-F4a-60-R124* shows the envelope of the MC results of onboard guidance trajectory re-computation considering the detected failure (*R4)* on top of the recovery strategies the red campaign already applied (*R1R2*).

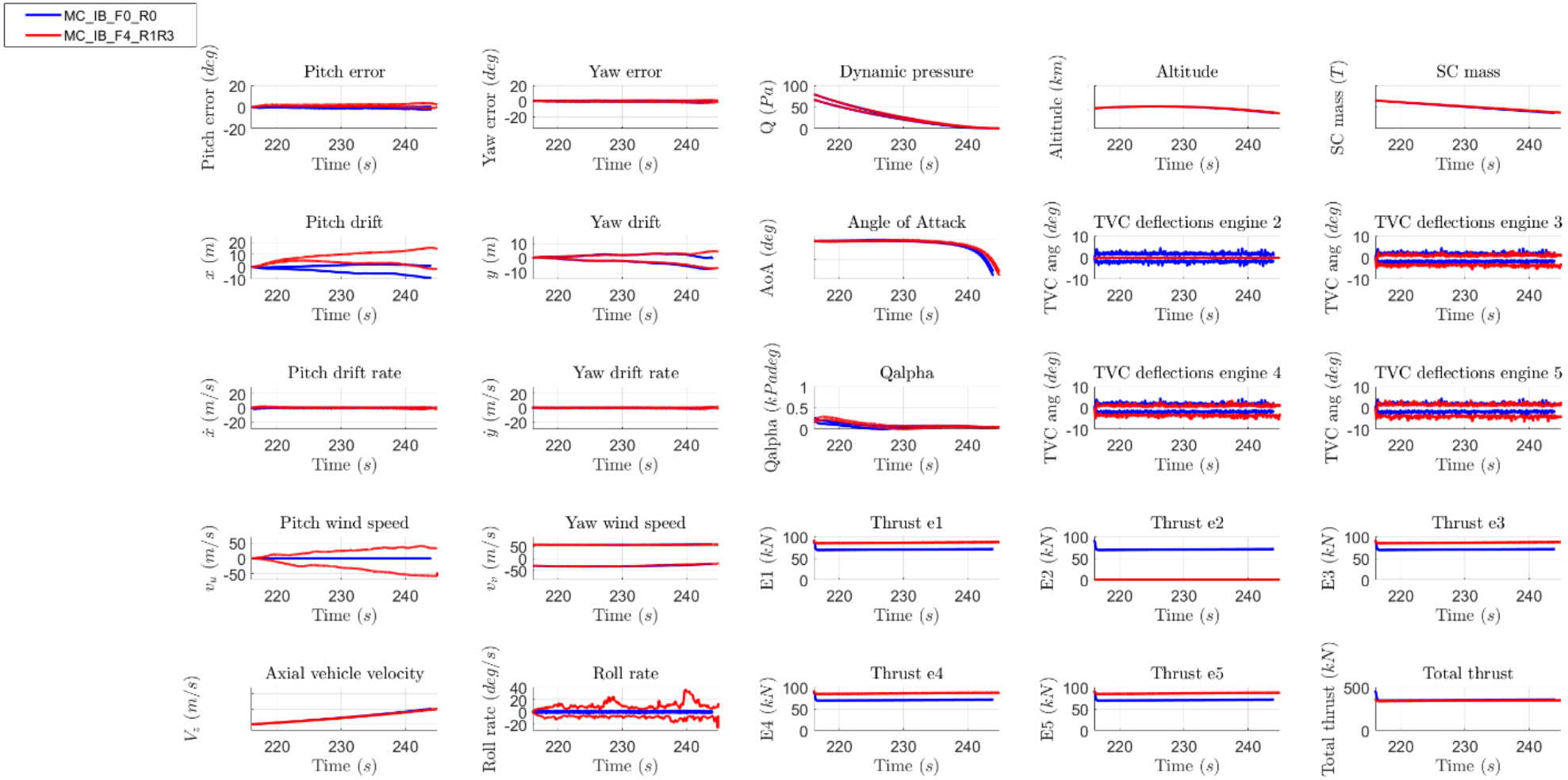

Figure 6 Envelopes of the time histories MC campaigns for 100 cases in Descent flight, during the IB propelled phase. In blue, *MC-IB-F0-R0* represents the baseline scenario without failures; in red, *MC-IB-F4-R1R3* shows the envelope of the results when a total loss of thrust type of failure occurs in an outer engine, the recovery action applied in this scenario is the dynamic TVC allocation (*R1*) and the change in TVC inner-loop control gains (*R3*).

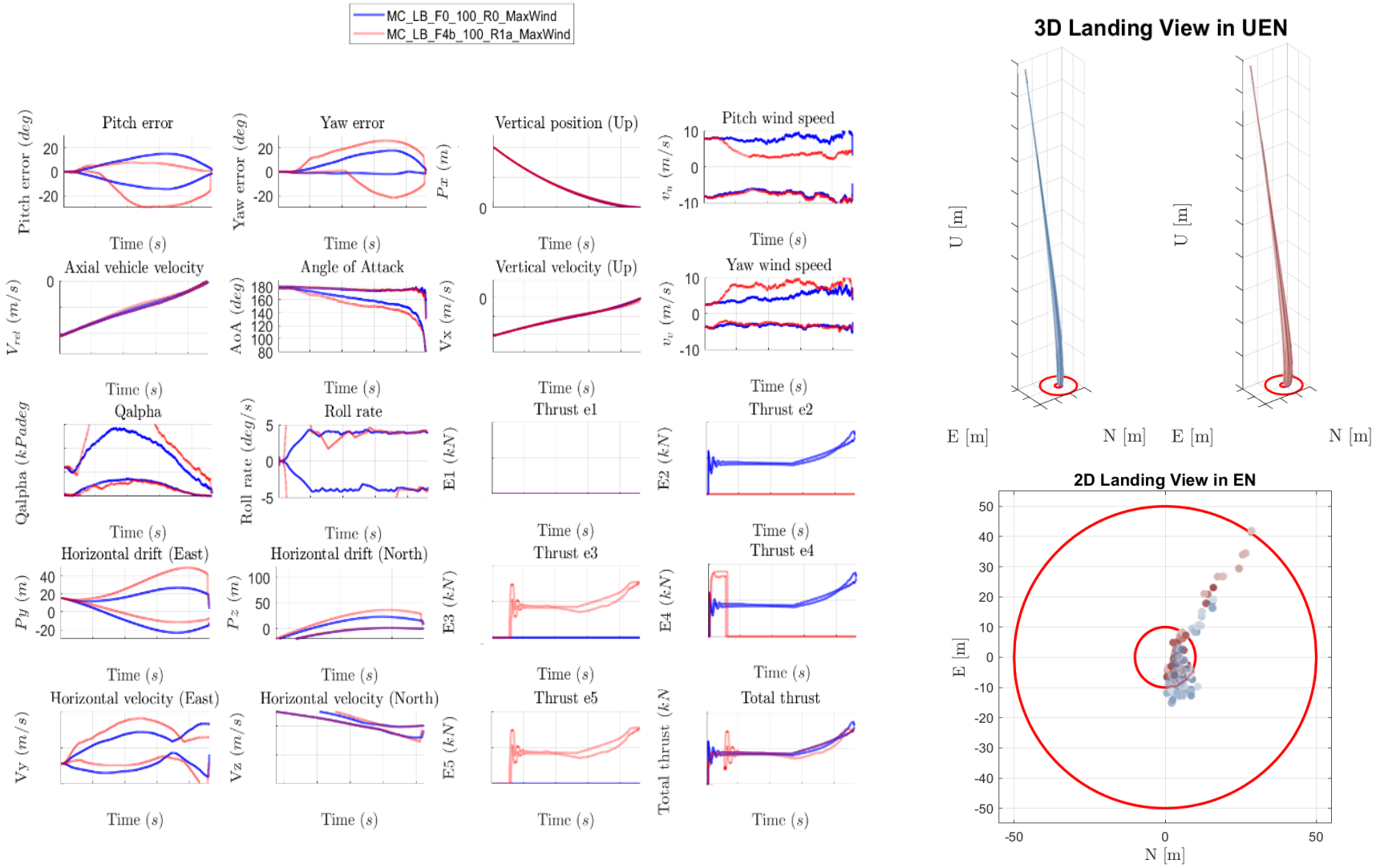

Figure 7 On the left, envelopes of the time histories MC campaigns for 100 cases in Descent flight, during the LB propelled phase. In blue, *MC-IB-F0-R0* represents the baseline scenario without failures; in red, *MC-IB-F4-R1R3* shows the envelope of the results when a total loss of thrust type of failure occurs in an outer engine, the recovery action applied in this scenario is the dynamic TVC allocation for thrust and torque recovery (*R1). On the right, 3D views of the LB maneuver for each case in the MC, accompanied by a 2D view of the end point of each case at the land site.**

6 Conclusion and future work

The outcomes of the activity "Fault-Tolerant Control of Clusters of Rocket Engines (FTC-CRE)" provide insights into the recovery capabilities of clusters of engines in the presence of propulsion/TVC failures and methodologies for Guidance and Control architectures with embedded fault-tolerant capabilities. The results provide the level of system degradation up to which the control reconfiguration can be effective, and from which a trajectory re-planning/re-targeting needs to be performed.

For the Ascent phase, the dynamic TVC allocation function R1 can provide recovery from propulsion failures up to 40% in a single engine and it can also cope with TVC jamming and loss of power. Beyond 40%, incorporating *R2* enhances robustness against the failure by design, notably reducing drift/drift-rate. *R3* addition did not show clear impact on the system. The use of the guidance reconfiguration *R4* in combination with *R1* and *R2* (i.e. *R124*) improved certain performance metrics, like attitude and aerodynamic loads, presenting lower peaks at maximum Qα region. However, conflict with the control function might appear and alter the controller performance. Finally, studying the impact of failure time revealed earlier failure degrades MECO performance, while later failure affects control performance.

For the Descent burns, the high thrust-to-weight ratio prompted the design of a thrust profile and characteristics of the propelled phases that account for failure reconfiguration at a guidance design level, allowing for redundancy to recover from the loss of thrust in a single engine. During the IB, failures in TVC actuation are more severe, particularly loss of power, resulting in instability. Hence, the suggested mitigation action is to shut off the engine, simplifying the issue to a total loss of thrust in a single engine, effectively addressed by *R1* and *R3*. As for the LB, complementing *R1* with dynamic thrust allocation (*R1**) is necessary for a soft-vertical landing. The most severe disturbance affecting the LB is the wind. This is mitigated by the trajectory's fault tolerance in its design, a LB targeted controller, and the action of *R1**, resulting in great performance at LP.

The SCvx technique for developing the algorithms for trajectory generation was chosen for its capabilities in on-board optimization. The developed version demonstrated the ability of SCvx to easily reconfigure for failures in Ascent. For both Ascent reconfiguration and Descent baseline, it provided feasible trajectories that closely replicated the FES simulator closed-loop dynamics with sufficient representativity, making it suitable for its aim. This project's application of SCvx to launcher guidance has opened a wide range of research lines to extend its advantages and enhance performance.

As for following extensions of this work, incorporating lateral forces minimization in the dynamic TVC allocation *R1* could enhance performance, especially in asymmetric scenarios, like failures or Descent burns. Additionally, the control design formulation proposed for *R2* can be tailored towards any of the other competing trade-off objectives during the Ascent flight (e.g. attitude, drift, aerodynamic loads) or used to achieve a trade-off balance for the best global performance. On the other hand, MECO conditions optimality modeling within SCvx for trajectory reconfiguration in Ascent *R4* can be further improved with exo-atmospheric flight optimization. To reduce possible interaction between onboard guidance computation and control, a co-design is suggested. Overall, propulsion failures pose a severe risk in the end-point performance, which could be mitigated at system level by an increase in the number of engines in the cluster or active fins. Active fins would greatly contribute to attitude tracking and stabilization in Descent, utilizing aerodynamics in its favor without the need for a launcher attitude command. This, coupled with the severity of the wind in the LB, could also benefit from a wind estimator.

Acknowledgements

This work is part of the project "Fault-Tolerant Control of Clustered Rocket Engines" (FTC-CRE) under a programe from and funded by, the European Space Agency, Contract No. 4000136228/21/NL/CRS. The view expressed in this paper can in no way be taken to reflect the official opinion of the European Space Agency.

References

[1] N. Paulino, et al. Fault Tolerant Control for a Cluster of Rocket Engines – Method and outcomes for guidance and control recovery strategies in launchers. In *Proceedings of the 12th International ESA Conference on Guidance, Navigation and Control Systems (ESA-GNC)*, 2023.

[2] Miramont Philippe. Ariane 5 on board software: redundancy management. In *Proceedings of the 2nd Embedded Real Time Software Congress (ERTS'04)*, 2004.

[3] Giannini M. and Irene Cruciani. VEGA LV Qualification process: GNC aspects on HWIL testing and analysis. In *Proceedings of the 5th European Conference for Aeronautics and Space Sciences*, 2013.

[4] Jeb S. Orr. and Tannen Van Zwieten. Robust, practical adaptive control for launch vehicles. In *Proceedings of the AIAA Guidance, Navigation, and Control Conference. American Institute of Aeronautics and Astronau*tics, 2012.

[5] Jeb S. Orr. and Nathan J. Slegers. High-Efficiency Thrust Vector Control Allocation. *Journal of Guidance, Control, and Dynamics, Vol. 37, No. 2*, 2014. DOI: 10.2514/1.61644

[6] John C. Doyle, Andrew Packard, and Kemin Zhou. Review of LFTs, LMIs, and mu. In *Proceedings of the 30th IEEE Conference on Decision and Control*, Brighton, UK, 1991, pp. 1227-1232 vol.2.

[7] Timothy M. Barrows and Jeb S. Orr. Dynamics and Simulation of Flexible Rockets. Academic Press, 2020.

[8] Diego Navarro-Tapia, et al. Structured H-infinity control design for the Vega launch vehicle: recovery of the legacy control behaviour. In *Proceedings of the 10th International ESA Conference on Guidance, Navigation and Control Systems (ESA-GNC)*, 2017.

[9] Pedro Simplicio, et al. New control functionalities for launcher load relief in ascent and descent flight. In *Proceedings of the 8th European Conference for Aeronautics and Aerospace Sciences, vol. 10,* 2019.

[10] Andrés Marcos, David Mostaza, and Luis F. Peñín. Achievable moments NDI-based fault tolerant thrust vector control of an atmospheric vehicle during ascent. In *Proceedings of the 7th IFAC symposium on fault detection, supervision and safety of technical processes, vol 42.8,* 2009.

[11] Diego Navarro-Tapia, et al. Legacy Recovery and Robust Augmentation Structured Design for the VEGA Launcher. *International Journal of Robust Nonlinear Control; 29:3363-3388,* 2019. DOI: 10.1002/rnc.4557

[12] Diego Navarro-Tapia. *Robust and Adaptive TVC Control Design Approaches for the VEGA Launcher*. PhD thesis, University of Bristol, 2019.

[13] Xinyuan Miao, et al. Successive Convexification for Ascent Trajectory Replanning of a Multistage Launch Vehicle Experiencing Nonfatal Dynamic Faults. *IEEE Transactions on Aerospace and Electronic Systems* 58.3, 2039-2052, 2021. DOI: 10.1109/TAES.2021.3133310

[14] Taylor P. Reynolds, et al. Dual quaternion-based powered descent guidance with state-triggered constraints. *Journal of Guidance, Control, and Dynamics*, 2020. DOI: 10.2514/1.G004536

[15] Michael Szmuk and Behcet Acikmese. Successive convexification for 6-DOF Mars rocket powered landing with free-final-time. In *Proceedings of AIAA Guidance, Navigation, and Control Conference*, 2018.

[16] Wei Zhang, Gan Tian, Zhigao Xu, and Zhengwei Yang. Failure characteristics analysis and fault diagnosis for liquid rocket engines. Vol. 233, no. 12. Cham, Switzerland: Springer, 2016.

[17] Christophe Roux and Irene Cruciani. Scheduling schemes and control law robustness in atmospheric flight of VEGA launcher. In Proceedings of the 7th ESA International Conference on Spacecraft Guidance, Navigation and Control Systems *(pp. 1*-5), June 2008.

[18] Pedro Simplicio. Guidance and Control Elements for Improved Access to Space. PhD thesis, University of Bristol, 2019.

Diego Navarro-Tapia, Andrés Marcos, Samir Bennani and Christophe Roux. Performance and robustness trade-off capabilities for the VEGA launcher TVC system. In *Proceedings of the 8th European Conference for Aeronautics and Aerospace Sciences, vol. 10,* 201